($Pn2_1m$, $Pnm2_1$, and $Pnmm$) were considered for solution of the structure. An examination of the Patterson map yielded a solution for the positions of the two rhodium atoms in $Pn2_1m$, but since the first difference map yielded too many phosphorus atoms, the other space groups were explored and rejected in turn. When we returned to $Pn2_1m$ (*bca* of No. 31; equivalent positions (x, y, z), $(x, y, -z)$, $(-x, {}^1/_2 + y, {}^1/_2 - z)$, $(-x, {}^1/_2 + y, {}^1/_2 + z)$) and included the phosphorus atoms in the structure factor calculation, nearly the entire tetraphenylborate group appeared in the difference map. With this encouragement, the remaining details of the structure were revealed by a combination of least-squares refinement and Fourier difference maps. A crystallographic mirror plane passes through the two terminal carbon monoxide ligands and the two rhodium atoms. Therefore one triphosphine ligand is in the asymmetric unit. The central phosphorus atom of this ligand is well-behaved, but two alternate sites exist for the terminal phosphorus atoms. These are occupied in a 1:1 mixture, which, on average, gives rise to the crystallographic mirror plane. An absorption correction was applied:[27] μ(Mo Kα) = 6.8 cm^{-1}; range of absorption correction factors 1.12-1.31. Atomic scattering factors and corrections for anomalous dispersion were from common sources.[28] Final blocked-cascade least-squares refinement was carried out on 213 parameters using 2845 reflections for which $I > 2\sigma(I)$. The Rh and P atoms were assigned anisotropic thermal parameters. Only those hydrogens not affected by the disordered phosphorus atoms were included. These were refined by using a riding model with C-H distance of 0.96 Å and U_{iso}(bonded C). The two largest peaks on a final difference map were 1.3 e Å^{-3}, near acetone and between P(1) and P(4). Refinement converged with $R = 0.053$, $R_w = 0.057$, and $w = [\sigma^2(F_o) + 0.0001F_o^2]^{-1}$. Table I gives the atomic coordinates; Tables II and III give selected interatomic distances and angles, respectively.

Acknowledgment. We thank the National Science Foundation, Grant CHE8217954, for financial support.

Registry No. 1, 99595-11-6; $[Rh_2(\mu\text{-dmmm})_2(CO)_2][BPh_4]_2 \cdot CH_3COCH_3$, 99595-10-5; $Rh_2(CO)_4(\mu\text{-Cl})_2$, 14523-22-9.

Supplementary Material Available: Tables of anisotropic thermal parameters, calculated hydrogen coordinates, and structure factors (18 pages). Ordering information is given on any current masthead page.

(27) The method obtains an empirical absorption tensor from an expression relating F_o and F_c: Hope, H.; Moezzi, B., Department of Chemistry, University of California, Davis CA, unpublished results.

(28) "International Tables for X-ray Crystallography"; Kynoch Press: Birmingham, England, 1974; Vol. 4.

Contribution from the Department of Chemistry, University of California, Davis, California 95616

^{1}H Nuclear Magnetic Resonance Studies of Iron(III) Porphyrin Complexes with Axial Aryl Ligands

Alan L. Balch* and Mark W. Renner

Received September 4, 1985

^{1}H NMR spectra of low-spin ($S = {}^1/_2$) iron(III) tetraarylporphyrin complexes bearing axial phenyl and *o*-, *m*-, and *p*-tolyl groups have been recorded and assigned. Addition of imidazole, 1-methylimidazole, 2-methylimidazole, 1,5-dimethylimidazole, and 1,4-dimethylimidazole to these five-coordinate complexes at -60 °C in chloroform gives six-coordinate adducts. The pattern of aryliron and porphyrin resonances remains the same in both the five- and six-coordinate adducts. Distinct resonances of the coordinated imidazole have been resolved and assigned. Analysis of the hyperfine shifts indicates π spin in the axial aryl groups of both five- and six-coordinate complexes and in the axial imidazole of the six-coordinate complexes. Comparisons of these results are made with the published spectra for the corresponding protein complexes derived from the arylhydrazine/dioxygen reaction with myoglobin. The patterns of resonances for phenyl, *p*-tolyl, and *m*-tolyl complexes are similar, but the model compound for the *o*-tolyl complex does not show the curious doubling of resonances, ascribed previously to restricted rotation, seen for *o*-tolylmyoglobin. Low-field resonances in the 40-20 ppm region of the protein spectra can now be assigned to histidine imidazole (2-H and 4-H) resonances.

Introduction

Iron(III) porphyrin complexes bearing an axial phenyl (or substituted phenyl) ligand have been established as key intermediates in the destruction of heme proteins by arylhydrazines.[1-3] Exposure of myoglobin to arylhydrazines in the presence of dioxygen leads to the eventual formation of *N*-arylprotoporphyrin IX.[4-6] The iron(III)-aryl intermediates have been directly observed by ^{1}H NMR spectroscopy.[1,2] The iron-bound phenyl group displays characteristic paramagnetically shifted resonances, which place the ortho and para resonances upfield at ca. -80 and -20 ppm and the meta resonance downfield at ca. 13 ppm at 25 °C. The three tolyl hydrazines also form corresponding iron-tolyl complexes with heme proteins. However, the *o*-tolyl derivative possesses a distinctly different chromophore[7-10] and an unusual ^{1}H NMR spectrum, which shows a doubling of resonances. This doubling has been interpreted to indicate the presence of two noninterconverting isomers.[2] Moreover the *o*-tolyl complex does not lead to the eventual formation of an N-substituted porphyrin.[6] In addition to extensive characterization by ^{1}H NMR spectroscopy,[1,2] phenylmyoglobin has been crystallized and subject to an X-ray diffraction study.[3] This study showed that the iron is six-coordinate and bound to the phenyl group and the proximal histidine imidazole as axial ligands.

Corresponding model complexes **1** are available from the reaction of Grignard reagents with iron(III) porphyrin halide complexes.[11-13] One such five-coordinate complex has been

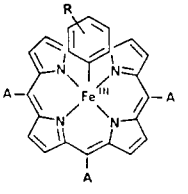

1

(1) Kunze, K. L.; Ortiz de Montellano, P. R. *J. Am. Chem. Soc.* **1983**, *105*, 1380.
(2) Ortiz de Montellano, P. R.; Kerr, D. E. *Biochemistry* **1985**, *24*, 1147.
(3) Ringe, D.; Petsko, G. A.; Kerr, D. E.; Ortiz de Montellano, P. R. *Biochemistry* **1984**, *23*, 2.
(4) Saito, S.; Hano, H. A. *Proc. Natl. Acad. Sci. U.S.A.* **1981**, *78*, 5508.
(5) Ortiz de Montellano, P. R.; Kunze, K. L. *J. Am. Chem. Soc.* **1981**, *103*, 6534.
(6) Augusto, O.; Kunze, K. L.; Ortiz de Montellano, P. R. *J. Biol. Chem.* **1982**, *257*, 6231.
(7) Huang, P.-K. C.; Kosower, E. M. *Biochim. Biophys. Acta* **1968**, *165*, 483.
(8) Itano, H. A. *Proc. Natl. Acad. Sci. U.S.A.* **1970**, *67*, 485.
(9) Itano, H. A.; Hirota, K.; Hosokawa, K. *Nature (London)* **1975**, *256*, 665.
(10) Itano, H. A.; Hirota, K.; Vedvick, T. S. *Proc. Natl. Acad. Sci. U.S.A.* **1977**, *74*, 2556.
(11) Ogoshi, H.; Sugimoto, H.; Yoshida, Z.-I.; Kobayashi, H.; Sakai, H.; Maeda, Y. *J. Organomet. Chem.* **1982**, *234*, 185.
(12) Cocolios, P.; Laviron, E.; Guilard, R. *J. Organomet. Chem.* **1982**, *228*, C39.

0020-1669/86/1325-0303$01.50/0

Table I. ^{1}H NMR Data for Iron(III) Complexes **1** in Chloroform-*d* Solutions (Chemical Shifts in ppm)

	Fe–phenyl				porphyrin phenyl				
compd	*o*	*m*	*p*	pyrrole	*o*	*o'*	*m*	*m'*	*p*
$C_6H_5Fe(TpTP)^b$ (−50 °C)	−111	20	−30	−28	2.5	0.07	3.8	3.3	−0.12[a]
$C_6H_5Fe(TMP)^c$ (−50 °C)	−102	21	−39	−28	1.2[a]	−0.5[a]	2.9		0.2[a]
p-$CH_3C_6H_4Fe(TPP)$ (−60 °C)	−113	23	89[a]	−30	2.3	−0.5	3.6	3.0	4.8
m-$CH_3C_6H_4Fe(TPP)$ (−60 °C)	−103, −105	17, −14[a]	−25	−30	2.4	−0.6	3.5	3.0	4.8
o-$CH_3C_6H_4Fe(TPP)$ (−60 °C)	−108, 80[a]	19, −2.8	−68	−22	4.6	2.5	4.9	4.5	5.9

[a] Methyl resonance. [b] TpTP is tetra-*p*-tolylporphyrin dianion. [c] TMP is tetramesitylporphyrin dianion.

characterized by an X-ray diffraction study.[14] Magnetic studies indicate that these iron(III) complexes are low spin ($S = {}^1/_2$).[15] The binding of pyridine to these five-coordinate complexes has been demonstrated.[16] The six-coordinate products retain the low-spin ($S = {}^1/_2$) character. During our studies[17] of the chemical oxidation[18-20] of **1** by one electron to form the corresponding phenyliron(IV) porphyrin complex, which is a transient intermediate that undergoes reductive elimination to produce an iron(II) complex of an N-substituted porphyrin as shown in eq 1, we collected a variety of new spectroscopic data on these

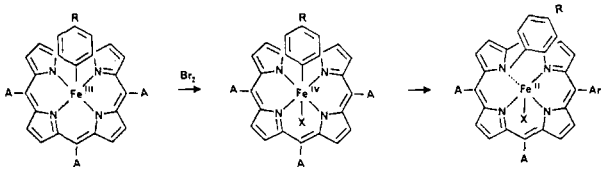

X = Br, ClO_4 (1)

iron(III)–phenyl complexes. Here we present a detailed analysis of the ^{1}H NMR spectra of these complexes with particular attention to their electronic structure and to comparison with data obtained on the corresponding intermediates observed in myoglobin.

Results

Five-Coordinate Complexes. The ^{1}H NMR spectra of four differently substituted forms of **1** are shown in Figure 1. Only those resonances shifted well outside the normal diamagnetic region are shown. These resonances include the pyrrole resonance of the porphyrin and all of the resonances of the phenyl or tolyl groups. The resonance assignments, which correspond to those made previously on the phenyl and *p*-tolyl model species,[13,16] are based on the intensity data and substitutional effects. Notice that the doubling of the ortho resonance for the *m*-tolyl derivative and the doubling of the meta resonance for the *o*-tolyl derivative are exactly what the lower aryl symmetry of these species requires. The significant differences in resonance positions of the pyrrole and para resonances for the *o*-tolyl resonance almost certainly reflects on the steric strain imposed on the iron–aryl bonding, with the Fe–C bond probably no longer perpendicular to the heme plane. Otherwise, the patterns of shifts for the four species are similar. Consequently all have similar electronic structures and all have aryl groups that freely rotate about the iron–carbon bonds. In particular the *o*-tolyl complex does not show the peculiar doubling of resonances that is present in *o*-tolylmyoglobin.[2]

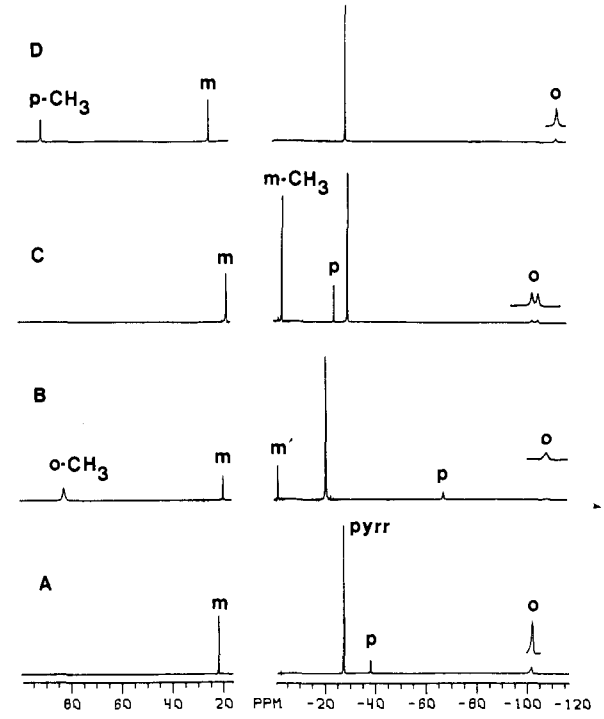

Figure 1. 360-MHz ^{1}H NMR spectra of various substituted forms of **1** in chloroform-*d* solution at −60 °C: A, phenyl; B, *o*-tolyl; C, *m*-tolyl; D, *p*-tolyl. The crowded diamagnetic envelope is not shown. Resonance assignments are as follows: pyrr, pyrrole protons; *o*, *m*, and *p*, phenyl(iron) protons, *o*-Me, *m*-Me, and *p*-Me, methyl phenyl(iron) protons.

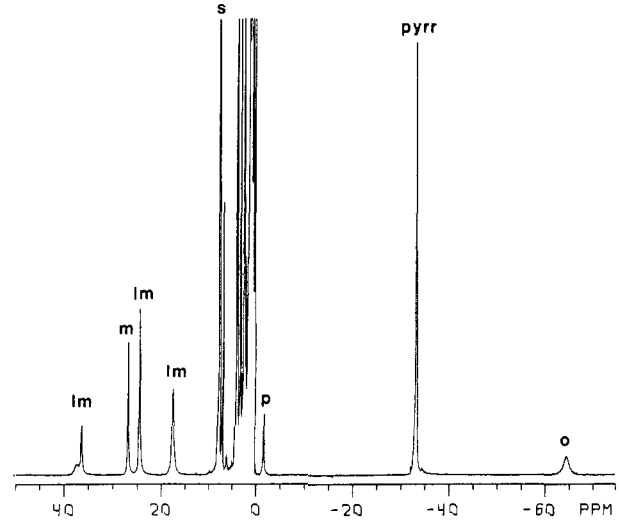

Figure 2. 360-MHz ^{1}H NMR spectrum of **1** (R = H, A = mesityl) (2 mM) in chloroform-*d* at −60 °C after the addition of excess 2,4-dimethylimidazole (5 mM). Resonances are labeled in accord with Figure 1; Im indicates resonances of coordinated imidazole, and s indicates the undeuterated solvent resonance.

The ^{1}H NMR data, including data for the aryl porphyrin substituents (A), for these and other related five-coordinate

(13) Cocolios, P.; Lagrange, G.; Guilard, R. *J. Organomet. Chem.* **1983**, *253*, 65.
(14) Doppelt, P. *Inorg. Chem.* **1984**, *23*, 4009.
(15) Recent studies have shown, however, that analogous tetraphenylporphyrin complexes with pentafluorophenyl or tetrafluorophenyl as axial ligands are high spin ($S = {}^5/_2$). Guilard, R.; Boisselier-Cocolios, B.; Tabard, A.; Cocolios, P.; Simonet, B.; Kadish, K. M. *Inorg. Chem.* **1985**, *24*, 2509.
(16) Lancon, D.; Cocolios, P.; Guilard, R.; Kadish, K. M. *Organometallics*, **1984**, *3*, 1164.
(17) Balch, A. L.; Renner, M. W. *J. Am. Chem. Soc.*, in press.
(18) Ortiz de Montellano, P. R.; Kunze, K. L.; Augusto, O. *J. Am. Chem. Soc.* **1982**, *104*, 3545.
(19) Mansuy, D.; Battioni, J.-P.; Dupré, D.; Sartori, E.; Chottard, G. *J. Am. Chem. Soc.* **1982**, *104*, 6159.
(20) Lancon, D.; Cocolios, P.; Guilard, R.; Kadish, K. M. *J. Am. Chem. Soc.* **1984**, *106*, 4472.

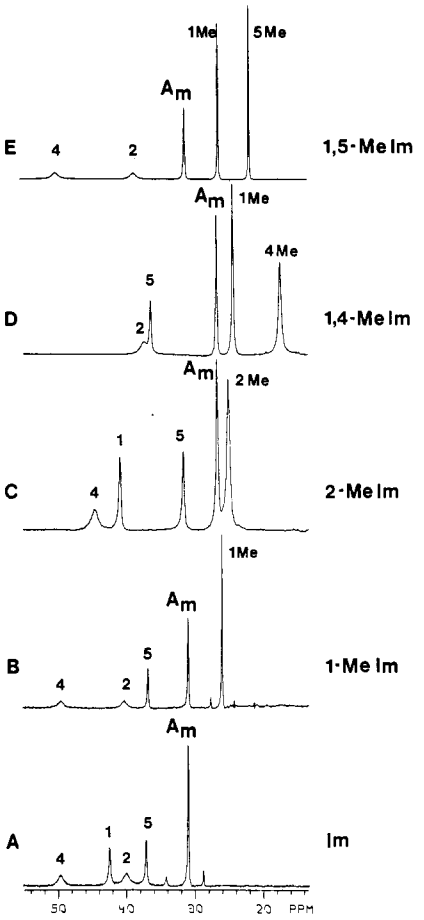

Figure 3. 360-MHz NMR spectra of **2** (A = mesityl) with various imidazoles in chloroform-*d* solution at −60 °C in the region of resonances of the coordinated imidazoles.

compounds are collected in Table I.

Six-Coordinate Imidazole Adducts. Addition of imidazole or methyl-substituted imidazoles to the iron(III) complex **1** results in the formation of six-coordinate adducts **2**. These are readily

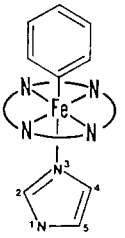

2

observed at −60 °C, but warming causes broadening of the resonances through exchange and at 25 °C the adduct **2** is largely dissociated to **1** under the conditions of our experiments. Figure 2 shows the ^{1}H NMR trace obtained after addition of 1,4-dimethylimidazole to **1** (A = mesityl, R = H). The pattern of porphyrin and phenyl resonances is similar to that found for **1**. That is the para phenyl(iron), pyrrole, and ortho phenyl(iron) resonances show increasing upfield shifts while the meta phenyl(iron) resonances are shifted downfield. However, comparison with the bottom trace of Figure 1 shows that the three iron–phenyl resonances are shifted significantly downfield upon formation of the adduct **2**. Similar downfield shifts are reported to occur on dissolving **1** in pyridine-d_5, where a 1:1 adduct has been spectroscopically characterized.[16] Additionally Figure 2 shows four resonances in the 40–10 ppm region, which can be assigned to the coordinated 1,4-dimethylimidazole. Integration of these resonances indicates that the two at 17.5 and 24.5 ppm are due to methyl groups (three protons/resonance) and the two resonances at ca. 37 ppm are due to single protons. Thus, one 1,4-dimethylimidazole is coordinated, and it is in slow exchange with free 1,4-dimethylimidazole at −60 °C.

Table II. Separation of the Isotropic Shifts into Contact and Dipolar Contributions for **1**

proton	$(\Delta H/H)_{iso}$	$(\Delta H/H)_{dip}$	$(\Delta H/H)_{con}$	rel GF[a]
o	−3.5	−3.5	0	1
		Fe–Phenyl		
o	−114	21	−135	−6.0
m	14.3	11.3	2.7	−3.2
p	−36	10.3	−46.3	−2.9
o-CH_3	79	−6.3	85.3	1.8
m-CH_3	−16	6.2	22.2	−1.75
p-CH_3	86	6.4	79.6	1.8

[a] GF is a geometric factor, $(3\cos^2\theta - 1)r^{-3}$.

The resonances of the coordinated bases can be assigned to individual protons on the basis of comparison of the set of substituted derivatives whose resonances are shown in Figure 3. The resonance assignments that follow from the substitutions are given over each resonance in the figure. The same general pattern for imidazole protons (with increasing downfield shifts in the order 5 < 2 < 1 < 4) is seen for all derivatives. Notice that the resonances of the 2- and 4-proton are broader (~500 Hz) than the resonances of the 1- and 5-protons (~200 Hz). The 2- and 4-protons are expected to be nearly equidistant from iron and closer to it than the 1- and 5-protons. Dipolar relaxation, which is expected to dominate the line widths, is therefore expected to preferentially broaden the 2- and 4-protons more than the 1- and 5-protons.

While the basic pattern of resonances is the same for all five imidazole derivatives, the two sterically encumbered ligands, 2-methylimidazole and 1,4-dimethylimidazole, produce spectra with significantly altered chemical shifts. Thus for these two axial bases the meta phenyl(iron) resonances show a 5–6 ppm upfield shift relative to the other base adducts. Likewise the 4-H resonance in trace C and 2-H and 5-H resonances in trace D show upfield shifts relative to their position in the unhindered derivatives in traces A, B, and E. These effects are all ascribed to tilting of the axial imidazoles for 2-methylimidazole and for 1,4-dimethylimidazole to minimize interaction of the 2- or 4-methyl groups with the porphyrin plane.

Discussion

Analysis of the Electronic Structure. The hyperfine shifts, the differences between the observed shifts for a paramagnetic complex, and the corresponding shifts of an analogous diamagnetic complex (in this case the In(III) analogue of **1**),[21] observed in the NMR spectra, are the sum of the scalar or contact contribution, which reflects the mode of spin delocalization, and the dipolar shift, which is due to the magnetic anisotropy of the iron. In the limit of axial symmetry, the dipolar shift is given by eq 2, where

$$\frac{\Delta H_{dip}}{H} = \frac{1}{3N}(\chi_{\parallel} - \chi_{\perp})\frac{3\cos^2\theta - 1}{r^3} \qquad (2)$$

N is Avogadro's number, $\chi_{\parallel}$ and $\chi_{\perp}$ are the magnetic susceptibilities parallel and perpendicular to the z axis (taken as coincident with the iron–phenyl bond), and r and θ are the usual polar coordinates.[22] Separation of the dipolar and contact terms can be made by examining a plot of the isotropic shift vs. the geometric factor, $(3\cos^2\theta - 1)r^{-3}$. This graph should yield a linear plot so long as the porphyrin aryl protons in **1** and **2** are effectively isolated (by virtue of their nearly perpendicular orientation to the porphyrin plane) from contact spin density within the iron/porphyrin core.[23]

(21) Cocolios, P.; Guilard, R.; Fournari, P. *J. Organomet. Chem.* **1979**, *179*, 311.
(22) Horrocks, W. D. In "NMR of Paramagnetic Molecules"; La Mar, G. N., Horrocks, W. D., Holm, R. H., Eds.; Academic Press: New York, 1973; pp 127–177.
(23) La Mar, G. N.; Walker (Jensen), F. A. In "The Porphyrins"; Dolphin, D., Ed. Academic Press: New York, 1979; Vol. 4, p 61.

Table III. Separation of the Isotropic Shifts into Contact and Dipolar Contributions for **2**

proton	$(\Delta H/H)_{obsd}$	$(\Delta H/H)_{iso}$	rel GF[a]	$(\Delta H/H)_{dip}$	$(\Delta H/H)_{con}$	$(\Delta H/H)_{con}$ for $PFe^{III}(Im)_2^{+}$[b]
			Porphyrin			
o	−0.5	−8.6	1	−8.6	0	0
o'	−1.2	−9.3	1	−8.6	−0.7	0
m	3.0	−4.76	0.46	−3.96	−0.8	~0
m'	2.9	−4.86	0.46	−3.96	−0.9	~0
p	3.9	−3.86	0.41	−3.5	−0.3	~0
p-CH_3	−1.2	−3.9	0.31	−2.7	−1.2	
pyrr	−34	−43	1.95	−17	−26	19.5[c]
			Iron–Phenyl[d]			
o	−69	−72	−6.0	52	−124	
m	30	24	−3.2	28	−4	
p	−8.8	−14.8	−2.9	25	−10.2	
			Imidazole			
1-H	42.2	29.5	−37.5	32.2	−3.2	−9.6
1-CH_3	25.7	24.1	−22.2	19.1	5.0	10.3
2-H	29.8	28.9	−60.0	51.6	−22.7	−28
2-CH_3	24.7	27.3	~0	~0	27.3	12
4-H	48.6	49.1	−50.8	49.9	−0.8	−8.2
4-CH_3	17.1	14.5	~0	~0	14.5	
5-H	36.9	32.5	−3.74	32.2	0.3	−7.6
5-CH_3	21.4	21.7	−2.14	18.4	3.3	9.0

[a] Relative geometric factors $(3\cos^2\theta - 1)r^{-3}$ from: La Mar, G. N.; Bold, T. J.; Satterlee, J. D. *Biochim. Biophys. Acta* **1977**, *498*, 189. [b] For $(Im)_2Fe^{III}P$ data from ref 23. [c] From ref 24. [d] Calculated from data in ref 14.

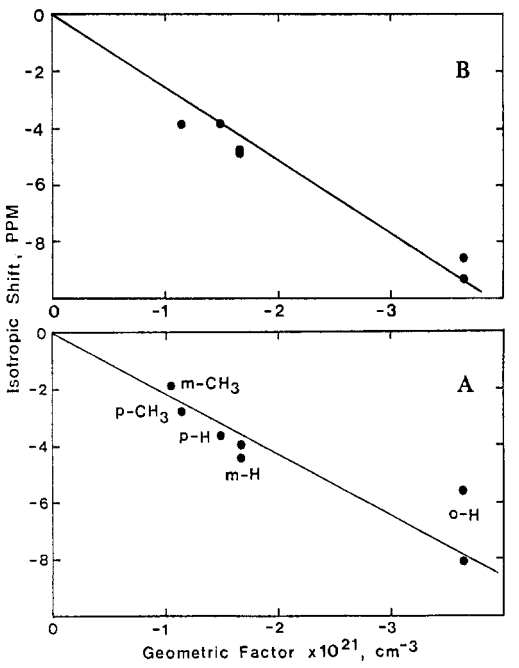

Figure 4. Plot of isotropic shifts for **1** (trace A) and **2** (trace B) at −60° in chloroform-*d* vs. the calculated geometric factor $(3\cos^2\theta - 1)r^{-3}$. Only resonances of porphyrin aryl groups (A) are plotted.

Such plots for **1** and **2** are shown in Figure 4. The linearity of these plots indicates effective isolation of the porphyrin aryl groups from unpaired spin delocalization and allows the separation of the contact and dipolar contributions. The results of this analysis are given in Tables II and III.

The contact shifts for the iron-bound aryl groups clearly indicate the presence of unpaired π-spin density on these aryl groups. The contact shifts for protons and methyl groups in the para as well as the ortho positions are of opposite sign but similar magnitude. Thus, this more thorough analysis confirms a previous interpretation[13] based on reversal of the isotropic shifts for the para proton and *p*-methyl group of these aryl ligands. Notice also that the contact shifts decrease in the order $o > p > m$ consistent with π-spin delocalization whereas attenuation with increasing distance from iron in the order $o > m > p$ is the expected characteristic of σ-spin delocalization. The presence of π spin on the aryl ligands is entirely consistent with the electronic structure of low-spin iron(III), which has the orbital occupancy $(d_{xy})^2(d_{xz},d_{yz})^3(d_{z^2})^0(d_{x^2-y^2})^0$ (with *z* perpendicular to the porphyrin plane) and therefore unpaired spin in an orbital of π symmetry with respect to metal–ligand bonding.

The porphyrin resonances of **1**, and **2** as well, are similar to those of other low-spin iron(III) complexes, particularly $PFe^{III}(Im)_2^{+}$[24,25] and $PFe^{III}(CN)_2^{-}$.[26] All show negligible π-spin density on the porphyrin-bound aryl groups and upfield shifted pyrrole resonances in very similar regions.

The pattern of imidazole contact shifts indicates the presence of unpaired π-spin density in this axial ligand. The contact shifts show clear evidence of reversal of sign for methyl substitution at the 1-, 2-, and 4-positions as expected for π-spin delocalization. Moreover the observed pattern of shifts is very similar to that seen in $PFe(Im)_2^{+}$[24] and substituted analogues. Comparative data are presented in Table III. The contact shifts for $PFe^{III}(Im)_2^{+}$ have previously been analyzed as being indicative of π-spin delocalization within the imidazole ligand.[24] The coordination of imidazole to **1** results in a decrease in the phenyl(iron) contact shifts (see Tables II and III). For the pyridine adduct of **1** similar observations were made and proposed to arise from pyridine acting as a π acceptor, therefore decreasing the π-spin delocalization into the phenyl(iron) group.[16] Our analysis of the contact contribution for the coordinated imidazole resonances confirm that this is the case for imidazole.

Comparison with Protein Analogues. The ^1H NMR spectra of arylmyoglobins derived from the reaction of myoglobin with arylhydrazines and dioxygen are characterized by large shifts for the aryl protons whereas the resonances of the porphyrin must lie in the crowded 20 to −5 ppm region.[1,2] Indeed the results of Lancon et al.[20] on $C_6H_5Fe^{III}OEP$ and $C_6H_5Fe^{III}OEP(py)$ (OEP is octaethylporphyrin dianion) indicate that the meso, methyl, and methylene porphyrin resonances will lie in the 10 to −5 ppm region. The iron–aryl resonance patterns observed in this study for phenyl, *p*-tolyl, and *m*-tolyl complexes completely agree with the published data[1,2] for the corresponding myoglobin complexes. However the spectrum for the *o*-tolyl complex **1** shows a simple spectrum indicative of free rotation about the Fe–C bond. This also holds for the more sterically encumbered complex **1** (R = *o*-CH_3, A

(24) Satterlee, J. D.; La Mar, G. N. *J. Am. Chem. Soc.* **1976**, *98*, 2804.
(25) La Mar, G. N.; Walker, F. A. *J. Am. Chem. Soc.* **1973**, *95*, 1782.
(26) Del Gaudio, J.; La Mar, G. N. *J. Am. Chem. Soc.* **1976**, *98*, 3014.

= mesityl). Thus the origin of the doubling of resonances in o-tolylmyoglobin must rest, as suggested by Ortiz de Montellano,[2] in o-tolyl-protein contacts and not in methyl-porphyrin interactions. From the spectrum of **1** (R = o-methyl, A = C_6H_5) we also conclude that the resonance corresponding to the upfield metaphenyl(iron) resonance is not detected in the o-tolylmyoglobin spectrum since it lies within the crowded diamagnetic region.

While the axial phenyl resonances in arylmyoglobin have been assigned in previous work,[1,2] the axial histidyl resonances have not been identified. On the basis of our observations on the six-coordinate adducts **2**, it can be expected that the 1-, 2-, and 4-imidazole histidine resonances will be shifted downfield from the crowded diamagnetic envelope into the 50–25 ppm region. Indeed the published spectra for phenylmyoglobin (Figure 1 of ref 1) and p- and m-tolylmyoglobin (Figure 2 of ref 2) do indeed show two resonances at ca. 30 ppm, which we believe can be assigned to the 2- and 4-protons of the axial histidine.

Experimental Section

Materials. The iron complexes **1** were prepared from the appropriate iron(III) porphyrin chloride and Grignard reagent by using an established procedure.[13] Unlike other derivatives, the o-tolyl complexes **1** were unstable particularly to column chromatography on silica gel. Therefore, these o-tolyl complexes (**1**, R = o-CH_3, A = C_6H_5 or mesityl) were generated by the reaction of o-tolylmagnesium bromide and the appropriate iron(III) complex directly in an NMR tube without further purification. All complexes were handled in a dioxygen-free, argon atmosphere in a glovebox. NMR spectra were run in deoxygenated chloroform-*d*. Imidazole adducts **2** were obtained by the addition (via a syringe) of a solution of the appropriate ligand in chloroform-*d* to a chloroform-*d* solution of **1**.

Instrumentation. NMR spectra were obtained on a Nicolet NT-360 FT spectrometer operating in the quadrature mode (^1H frequency 360 MHz). Between 200 and 1000 transients were accumulated over a 40-kHz bandwidth with 16K data points and a 6-μs 90° pulse. The signal-to-noise ratio was improved by apodization of the free induction decay, which introduced a negligible 3–10 Hz of line broadening. The peaks were referenced against tetramethylsilane.

Acknowledgment. We thank the National Institutes of Health (Grant GM26226) for support.

Registry No. $C_6H_5Fe(TpTP)$, 87607-84-9; $C_6H_5Fe(TMP)$, 99726-42-8; p-$CH_3C_6H_4Fe(TPP)$, 87621-56-5; m-$CH_3C_6H_4Fe(TPP)$, 99784-41-5; o-$CH_3C_6H_4Fe(TPP)$, 99726-43-9; 1,5-Me_2Im, 99726-44-0; 1,4-Me_2Im, 99726-45-1; 2-MeIm, 99726-46-2; 1-MeIm, 99726-47-3; Im, 99726-48-4.

Contribution from the Department of Chemical, Biological, and Environmental Sciences, Oregon Graduate Center, Beaverton, Oregon 97006-1999

Resonance Raman Spectroscopic Evidence for Perturbation of Vinyl Modes in Copper(I)-Protoheme π-Complexes

Scott S. Sibbett, Thomas M. Loehr, and James K. Hurst*

Received June 24, 1985

Copper(I) addition to aqueous micellar suspensions of ferriprotoporphyrin or its dimethyl ester causes perturbation of resonance-enhanced Raman bands associated with vibrational motions of the vinyl group substituents at the 3- and 8-positions of the porphyrin ring. No spectral perturbations occur upon adding cupric, zinc, or hexaaquochromic ions to these heme solutions or upon adding Cu(I) to ferrideuteroporphyrin. The data are interpreted to indicate Cu(I) coordination at the vinyl positions. Consistent with this view, intensity is lost in the vinyl carbon–carbon stretching region at 1615–1630 cm^{-1} and a new intensity appears at ~1530 cm^{-1}, assignable to the carbon–carbon stretch of Cu(I) π-complexed olefin bonds. Similar changes occur in this region upon reduction of oxidized cytochrome oxidases of both mitochondrial and microbial origin, suggesting that the peripheral vinyl substituents on the heme may form part of the Cu(I) ligation environment in the reduced copper–heme binuclear center comprising the oxygen reductase site.

Introduction

Protoporphyrin IX has two peripherally bound vinyl groups. The influence of these groups upon the physicochemistry of the porphyrin core is illustrated by comparing a series of deuteroporphyrins with zero, one, or two vinyl substituents. Such a series exhibits, for example, progressive red-shifting of electronic bands with increasing substitution (Figure 1).[1-3] This incremental shifting indicates that both vinyl groups conjugate with the porphyrin aromatic system; bathochromism indicates that they influence porphyrin electronic states in the expected $\pm E$ electromeric manner.[4,5] Vinyl groups also affect porphyrin vibrational properties in various ways that generally increase the number of detectable bands. Since vinyl vibrational modes are vibronically active in porphyrin electronic transitions, laser excitation within these transitions produces resonance Raman enhancement of both vinyl and porphyrin skeletal modes.[6-8] Resonance coupling occurs between some vinyl and porphyrin fundamental modes, causing band splitting and frequency shifts, which identify the coupled motions.[8,9] Attachment of the vinyl groups at the asymmetric 3,8-positions[10] in protoporphyrin IX causes symmetry lowering, which can induce Raman activity into porphyrin E_u modes forbidden under D_{4h} symmetry. Several such E_u bands have been assigned in the spectra of nickel(II) and iron(III) protoporphyrin IX.[9,11]

The modification of porphyrin physicochemistry by vinyl substituents may be important to the function of many protoheme proteins, e.g. in modulating the oxygen affinities of O_2-binding

* To whom correspondence should be addressed.

(1) Pruckner, F. *Z. Phys. Chem., Abt. A* **1942**, *190*, 101–125.
(2) Falk, J. E.; Perrin, D. D. "Haematin Enzymes"; Falk, J. E., Lemberg, R., Morton, R. K., Eds.; Pergamon Press: Oxford, England, 1961; Part 1, pp 56–71.
(3) Falk, J. E. "Porphyrins and Metalloporphyrins"; Elsevier: Amsterdam, 1964; pp 77–84.
(4) Djerassi, C.; Lu, Y.; Walsh, A.; Shu, A. Y. L.; Goldbeck, R. A.; Kehres, L. A.; Crandell, C. W.; Wee, A. G. H.; Kniezinger, A.; Gaete-Holmes, R.; Loew, G. H.; Clezy, P. S.; Bunnenberg, E. *J. Am. Chem. Soc.* **1984**, *106*, 4241–4258.
(5) Dewar, M. J. S.; Dougherty, R. C. "The PMO Theory of Organic Chemistry"; Plenum: New York, 1975; pp 413–417.
(6) Albrecht, A. C. *J. Chem. Phys.* **1961**, *34*, 1476–1484.
(7) Spiro, T. G.; Strekas, T. C. *J. Am. Chem. Soc.* **1974**, *96*, 338–345.
(8) Adar, F. *Arch. Biochem. Biophys.* **1975**, *170*, 644–650; **1977**, *181*, 5–7.
(9) Choi, S.; Spiro, T. G.; Langry, K. C.; Smith, K. M. *J. Am. Chem. Soc.* **1982**, *104*, 4337–4344.
(10) Nomenclature conforms to the recommendations of: Bonnett, R. *Porphyrins* **1978**, *1*, 9–14.
(11) Choi, S.; Spiro, T. G.; Langry, K. C.; Smith, K. M.; Budd, D. L.; La Mar, G. N. *J. Am. Chem. Soc.* **1982**, *104*, 4345–1351. Choi, S.; Spiro, T. G. *J. Am. Chem. Soc.* **1983**, *105*, 3683–3692.

0020-1669/86/1325-0307$01.50/0